Eurasian Journal of Physics and Functional Materials

Volume 5 | Number 3

Article 9

Pages: 242 - 250

9-22-2021

Features of model thin-film solar cells photoelectric characteristics based on a non-toxic multi-component connection $CuZn_2AlS_4$

D. Sergeyev
Begeldinov Aktobe Aviation Institute; Zhubanov Aktobe Regional University ,Kazakhstan

K. Shunkeyev
Zhubanov Aktobe Regional University ,Kazakhstan

B. Kuatov
Begeldinov Aktobe Aviation Institute ,Kazakhstan

N. Zhanturina
Zhubanov Aktobe Regional University ,Kazakhstan ,

Recommended Citation

Sergeyev, D.; Shunkeyev, K.; Kuatov, B.; and Zhanturina, N. (2021) "Features of model thin-film solar cells photoelectric characteristics based on a non-toxic multi-component connection $CuZn_2AlS_4$," *Eurasian Journal of Physics and Functional Materials*: Vol. 5: No. 3, Article 9.
DOI: https://doi.org/10.32523/ejpfm.2021050309

Eurasian Journal of Physics and Functional Materials

2021, 5(3), 242-250

Features of model thin-film solar cells photoelectric characteristics based on a non-toxic multi-component connection $CuZn_2AlS_4$

D. Sergeyev*[,1,2], K. Shunkeyev[2], B. Kuatov[1], N. Zhanturina[2]

[1]Begeldinov Aktobe Aviation Institute, Aktobe, Kazakhstan

[2]Zhubanov Aktobe Regional University, Aktobe, Kazakhstan

E-mail: serdau@mail.ru, shunkeev@rambler.ru

DOI: **10.32523/ejpfm.2021050309**
Received: 05.08.2021 - after revision

In this paper, the features of the characteristics of model thin-film solar cells based on the non-toxic multicomponent compound $CuZn_2AlS_4$ (CZAS) are considered. The main parameters (open-circuit voltage, short-circuit current, fill factor, efficiency) and characteristics (quantum efficiency, current-voltage characteristic) of thin-film solar cells based on CZAS have been determined. The minimum optimal thickness of the CZAS absorber is found (1-1.25 microns). Deterioration of the performance of solar cells with an increase in operating temperature (280-400 K) is shown. It is revealed that in the wavelength range of 390-500 nm CZAS has a high external quantum efficiency, which allows its use in designs of multi-junction solar cells designed to absorb solar radiation in the specified range. It is shown that the combination of CZAS films with a buffer layer of non-toxic ZnS increases the performance of solar cells.

Keywords: thin film solar cell, $CuZn_2AlS_4$ (CZAS), electrical properties, quantum efficiency, SCAPS

Introduction

In recent years, renewable energy sources have been used to solve environmental problems [1]. The most economical and efficient type of renewable energy

source is solar energy. Recently, active work is underway to introduce alternative sources of electricity in various industries based on photovoltaic modules that use solar energy [2]. Despite the wide production of silicon-based solar cells, other materials are intensively used to improve the output energy characteristics of photovoltaic modules (see, for example, [3-5]). The search and synthesis of new materials with unusual properties, used to create new types of solar cells, and the modernization of the properties of existing types of solar cells by improving the technology of their manufacture and processing will mainly determine the progress in solar energy.

Currently, work is underway to study thin-film solar cells (TFSC) based on both inorganic and organic semiconductor absorbers. The leading "absorbing" material for creating TFSC is a quaternary copper compound with a chalcopyrite structure $Cu(In,Ga)(S, Se)_2$ (CIGS) [6-8]. TFSCs based on CIGS have high absorption coefficients and are relatively cheap. We also note that due to the optimal values of the absorption coefficients of CIGS in the range from $3 \cdot 10^5$ cm^{-1} to $6 \cdot 10^6$ cm^{-1}, CIGS film with a thickness of 1-4 μm is sufficient for effective absorption [9]. However, despite the above advantages, TFSCs based on CIGS are inferior to their counterparts in efficiency and radiation resistance, and the elements In and Ga included in CIGS are highly toxic substances. In order to avoid the expensive disposal of such toxic elements for the creation of TSE, a search is underway for environmentally friendly materials with improved photovoltaic properties. By replacing highly toxic elements In, Ga, respectively, with non-toxic elements Zn, Sn, a multicomponent semiconductor compound $Cu_2ZnSn(S, Se)_4$ (CZTS) was obtained [10-12]. CZTS films have a low quantum efficiency in the range of relatively short wavelengths. Currently, a search is underway for various semiconductor materials with the highest external quantum yield in a wide wavelength range. In [13], the optical properties of the multicomponent compound $CuZn_2AlS_4$ (CZAS) are given, which can be used as an alternative absorbing material to CZTS. CZAS, like CZTS, is a non-toxic and cheap material.

Usually, CdS layers are used as a buffer layer in TFSCs. However, due to their relatively high toxicity, such solar cells cannot be environmentally friendly. In addition, the band gap of CdS is 2.4 eV, which is low and ineffective for the buffer layer. A good alternative for the CdS buffer layer is non-toxic ZnS films, which, due to their large band gap, transmit light in the near ultraviolet region [14].

This paper presents the results of modeling TFSCs based on a non-toxic multicomponent semiconductor compound CZAS with a ZnS buffer layer, determines their main photoelectric characteristics, and presents the results of comparison with TFSCs based on CZTS.

Simulation Model and Methods

The geometry of TFSC based on the CZAS absorber is shown in the inset in Figure 1. The TFSC core consists of ZnO, ZnS and CZAS. The layer thicknesses are shown in Figure 1. To increase the efficiency of TSC, n type semiconductors

(ZnO, ZnS) are separated from the p-type semiconductor (CZAS) by a 15 nm layer of ordered vacancy compound (OVC) [15]. When calculating the OVC, the following parameters were described: Bandgap 1.72 eV, Electron affinity 4.5 eV, Dielectric permittivity (relative) 10, Conduction band effective density of states $1.7 \cdot 10^{19}$ cm^{-3}, Valence band effective density of states $2.4 \cdot 10^{18}$ cm^{-3}.

In this work, the evaluation of the output parameters of TFSC based on the CZAS absorber was carried out in the SCAPS (Solar Cell Capacitance Simulator) program developed by the Department of Electronics and Information Systems (ELIS) of the University of Ghent [16-19]. Using the SCAPS program, the output parameters of multicomponent TFSCs ZnO/ZnS/OVC/CZAS and ZnO/CdS/OVC/ CZAS have been simulated. To simulate the properties of TFSC, the following parameters of the CZAS absorbing material were used: Bandgap 1.66 eV, Electron affinity 4.1 eV, Dielectric permittivity (relative) 6.4, Conduction band effective density of states $2.2 \cdot 10^{18}$ cm^{-3}, Valence band effective density of states $1.8 \cdot 10^{19}$ cm^{-3}.

The calculation of the photoelectric parameters of the TFSC was carried out by numerical solving the basic equations of the semiconductor (Poisson's equation, which connects the electrostatic potential with the total charge density):

$$\frac{\partial}{\partial x} = \left(\varepsilon_0 \varepsilon_r \frac{\partial \psi}{\partial x} \right) = -e \left(p - n - N_D^+ - N_A^- + \frac{\rho_{def}}{e} \right), \quad (1)$$

where ψ – electrostatic potential, ε_r – semiconductor dielectric constant, N_D^+ – ionized donor concentration, N_A^- – ionized acceptor concentration, p – free holes concentration, n – free electrons concentration, ρ_{def} – defect charge density.

Drift and diffusion mechanisms of charge carrier transport in semiconductors are described, respectively, by the following equations:

$$J_n = D_n \frac{dn}{dx} + \mu_n n \frac{d\phi}{dx}, \quad (2)$$

$$J_p = D_p \frac{dp}{dx} + \mu_p p \frac{d\phi}{dx}, \quad (3)$$

where J_n and J_p – current density of electrons and holes, D_n and D_p – diffusion coefficients of electrons and holes, ϕ – electric field, μ_n and μ_p – mobility of electrons and holes, respectively.

It is known that the efficiency of TSE, regardless of the design and materials used, is assessed by parameters such as open circuit voltage (V_{oc}), short-circuit current (I_{sc}), fill factor (FF) and efficiency (η) [20].

Open circuit voltageis determined by next equation:

$$V_{oc} = \frac{k_B T}{q} \ln \left(1 + \frac{J_{ph}}{J_0} \right), \quad (4)$$

where J_{ph} – photocurrent density, J_0 – dark current density, $k_B T/q$ – thermal potential, k_B – Boltzmann constant, T – temperature.

The short-circuit current is determined by the formula:

$$J_{sc} = q \mu_d n E, \quad (5)$$

where μ_d – charge carrier drift mobility, n – photogenerated charge carrier density, E – electric field strength.

The fill factor is defined as the ratio of the maximum power of the TSE to the product and determines the maximum power at the TFSC output:

$$FF = \frac{P_{\max}}{V_{oc} I_{sc}}. \tag{6}$$

Efficiency is the ratio of the power generated by the TFSC to the power of the incident solar radiation:

$$\eta = \frac{P_{\max}}{P_{in}} = \frac{V_{oc} I_{sc} FF}{P_{in}}. \tag{7}$$

The external quantum efficiency of the model TFSC is determined by the formula:

$$QE = \frac{J_{ph}(\lambda)}{eF(\lambda)}, \tag{8}$$

where $J_{ph}(\lambda)$ – total photogenerated current density, $F(\lambda)$ – solar stream. Solar radiation AM 1.5 with a power density of 100 $\mathrm{mW/cm^2}$ is used as a source of sunlight. Note that the SCAPS software calculates the photovoltaic parameters based on Shockley-Reed-Hall recombination statistics. The basic SCAPS equations are described in detail in [16-19].

Results and Discussions

It is known that the mobility of electrons is greater than the mobility of holes; therefore, to increase the efficiency, the TFSC layer from a *p*-semiconductor is structurally made thicker than the layer of an *n*-semiconductor. This is done so that an approximately equal number of electrons and holes in the corresponding layers, without undergoing recombination, can reach the electrodes at the same time. Therefore, when calculating the TFSC, one of the important tasks is to find the optimal value of the absorber thickness. Figure 1 shows the behavior of the dependence of the quantum efficiency of the TFSC on the wavelength with an increase in the absorber thickness from 0.5 μm to 3 μm at a temperature of 300 K. At an absorber thickness of 1 μm and more, the external quantum efficiency is stabilized. According to the JV characteristic, it can be seen that the thicker the absorber, the better the current capability of the TSE (Figure 2), although the current density is stabilized at an absorber thickness of 1 μm and higher.

In Figure 3 the results of calculations to assess the effect of the CZAS absorber thickness on the TFSC parameters are shown. The thickness of the absorber layer was varied from 0.5 μm to 3 μm with a step of 0.25 μm. The open circuit voltage is set at 1.026 V with a layer thickness of 1 micron and above (Figure 3 a). The short-circuit current density at an absorber thickness of 1-3 microns changes insignificantly from 15.252 $\mathrm{mA/cm^2}$ to 15.372 $\mathrm{mA/cm^2}$ (Figure 3 b). The fill factor in the range from 0.5 μm to 1.25 μm rapidly drops from 59.83% to 55.92%, then it stabilizes and takes on a value of 55.83%. The efficiency grows with increasing thickness, but the increase in efficiency becomes insignificant at a

thickness of 1 μm and more, since in the range 1-3 μm the efficiency varies from 8.79% to 8.8%. Thus, the calculation results show that the minimum optimal thickness of the CZAS absorber is 1-1.25 microns.

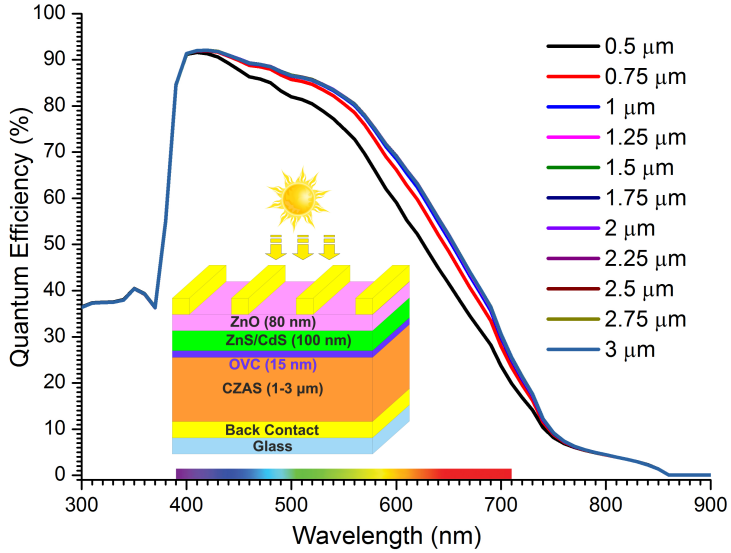

Figure 1. Dependence of the quantum efficiency of TFSC based on CZAS on wavelength and its schematic structure.

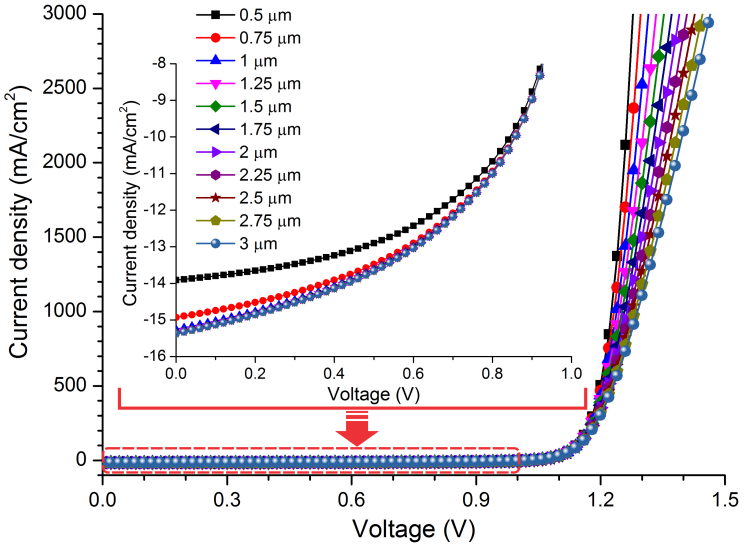

Figure 2. JV-characteristic of TFSC based on CZAS (in the inset - JV-characteristic in the range of 0-1 V).

The influence of the operating temperature on the external quantum efficiency of the JV characteristic of the TFSC is shown in Figures 4, 5, respectively. The temperature value varied from 280 K to 400 K with a rise rate of 20 K. As you can see, with an increase in the operating temperature, the quantum efficiency decreases. Especially, a noticeable decrease in QE is observed in the range of relatively short wavelengths from 300 nm to 370 nm (Figure 4). An increase in temperature leads to a deterioration of the JV characteristics of TFSCs, and their productivity decreases significantly (Figure 5).

Figure 6 shows the results of calculating the assessment of the effect of temperature on the parameters of the TFSC. We observe that with increasing

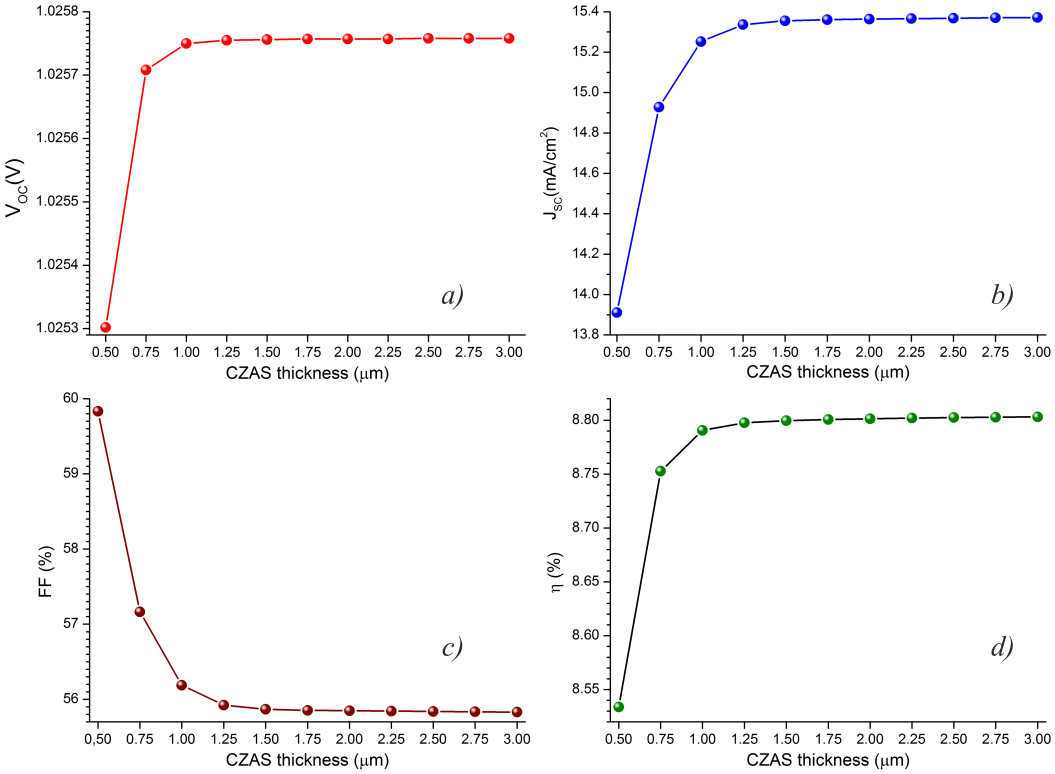

Figure 3. Influence of CZAS absorber thickness on TFSC parameters: a) V_{OC} ; b) J_{SC} ; c) FF; d) η.

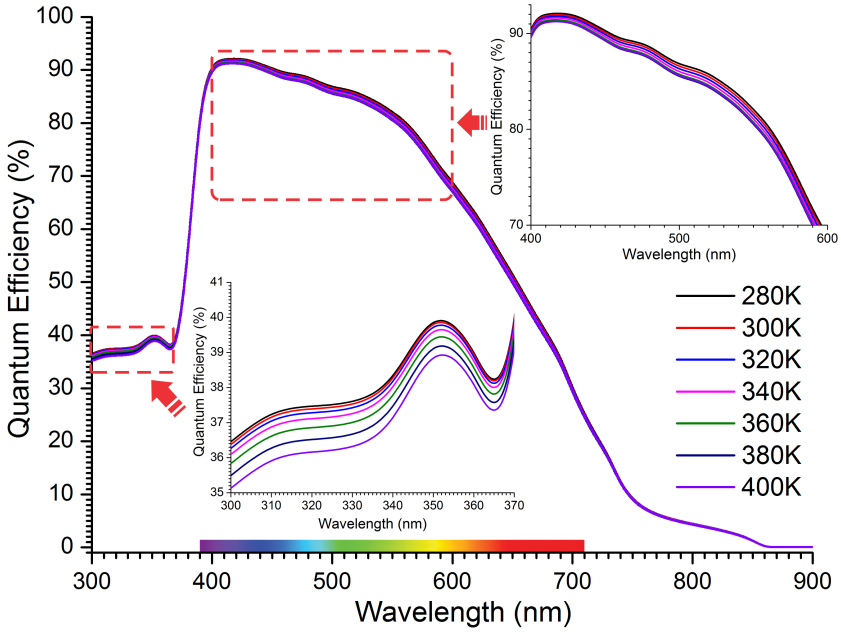

Figure 4. Evolution of the quantum efficiency of TFSC based on CZAS with increasing temperature.

temperature, the open circuit voltage of the TFSC decreases, and the short-circuit current density increases. Note that JSC in the range of 280-320 K falls insignificantly from the level of 15.32 mA/cm^2 to 15.2 mA/cm^2 and its value depends on the material of the absorber. The fill factor ranges from 55.38% to 56.98%. In the range of working temperatures of 300-360 K, its value decreases intensively. The minimum FF value is observed at a temperature of 360 K. The

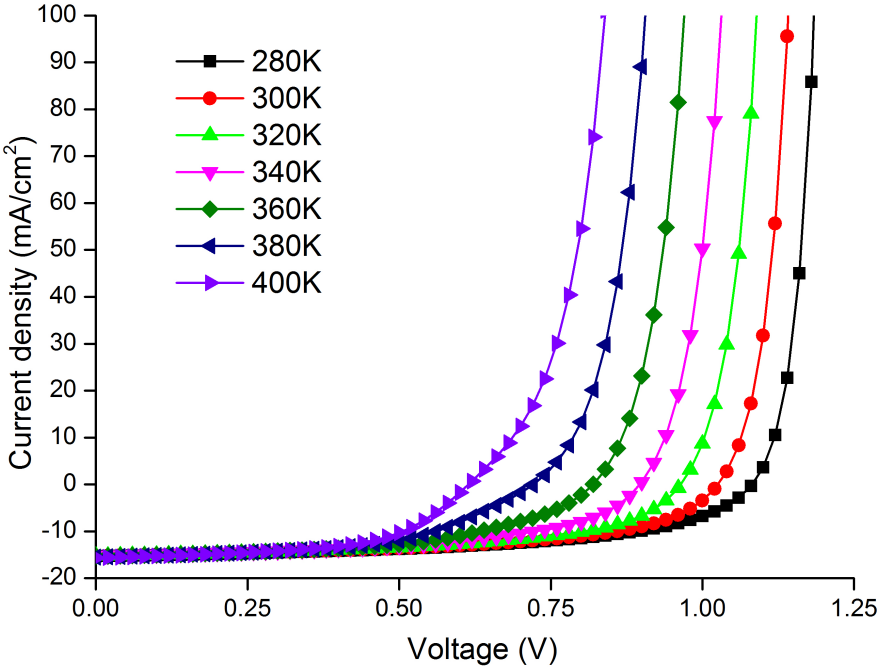

Figure 5. Evolution of the JV characteristic of TFSC based on CZAS with increasing temperature.

efficiency of the considered model TFSC rapidly decreases with an increase in temperature from 9.2% to 5.47%, its maximum value is observed at 280 K. As you can see, the main characteristics and parameters of TFSC based on CZAS decrease with an increase in the operating temperature, since an increase in temperature will lead to to a decrease in the band gap of semiconductors, and also an increase in the fraction of lattice scattering, as a result of which the mobility of charge carriers decreases, the concentrations of the majority charge carriers change significantly, and the probability of recombination of an electron-hole pair increases. Such changes lead to a decrease in efficiency.

Figure 7 shows a comparison of the quantum efficiency and JV characteristics of model TFSCs based on CZTS/CdS, CZTS/ZnS and CZAS/CdS, CZAS/ZnS.

In the wavelength range of 390-500 nm, a deterioration in the quantum efficiency of TFSC is observed based on the combination of CZTS, CZAS absorbers with a CdS buffer layer up to 62% and 66%, respectively. Replacing the CdS buffer layer with ZnS improves the quantum efficiency of the TFSC in the indicated short-wavelength region. The increase in the quantum efficiency of CZTS/ZnS, CZAS/ZnS to 82% and 92%, respectively, in the violet-blue range, is explained by a decrease in the loss of absorption of photons in the ZnS layer [20]. Despite the improved quantum efficiency of CZAS/ZnS in the range of 390-500 nm, in the range from 540 nm and higher, CZAS/ZnS is significantly inferior to CZTS. Due to this, the efficiency of TFSC based on CZAS/ZnS and CZAS/CdS is lower (8.8% and 6.72%, respectively) than the efficiency based on CZTS/ZnS and CZTS/CdS (11.62% and 12.1%, respectively). These features of the quantum efficiency are reflected in the JV-characteristic of the TFSC. We observe an improvement in CVC of the TFSC with the CZAS/ZnS absorber as compared to the CZAS/CdS, which shows a good agreement of the CZAS film with the ZnS buffer layer.

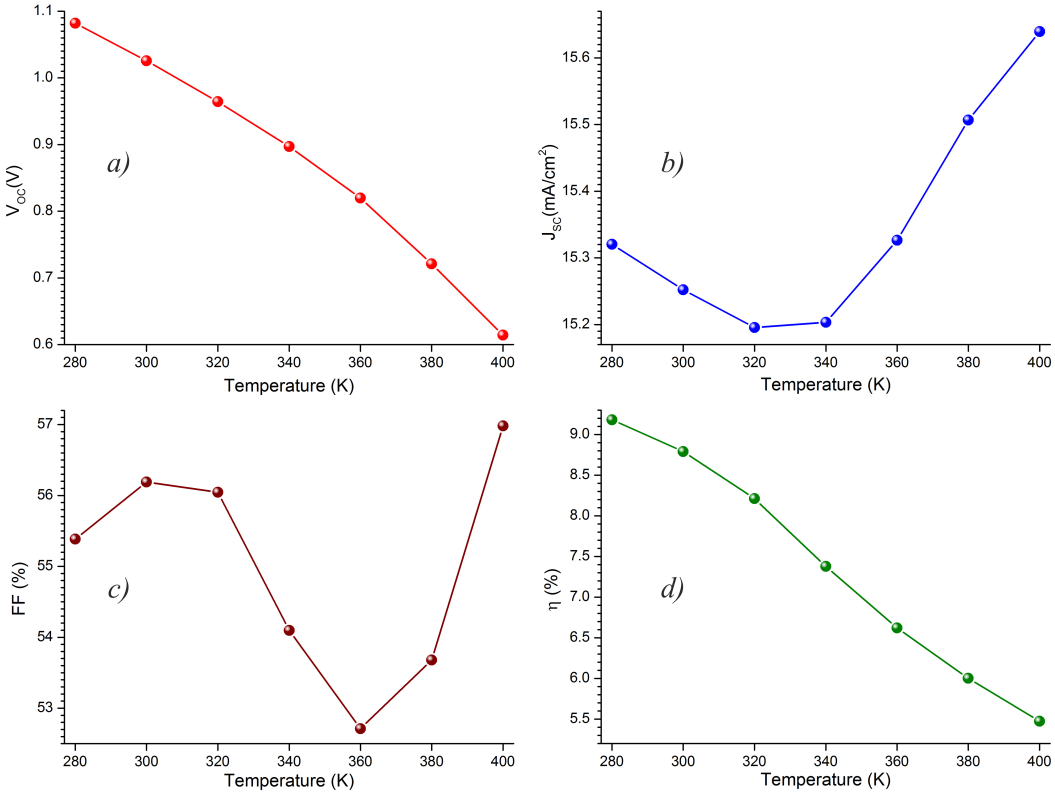

Figure 6. Influence of temperature on TFSC parameters: a) V_{OC} ; b) J_{SC} ; c) FF; d) η.

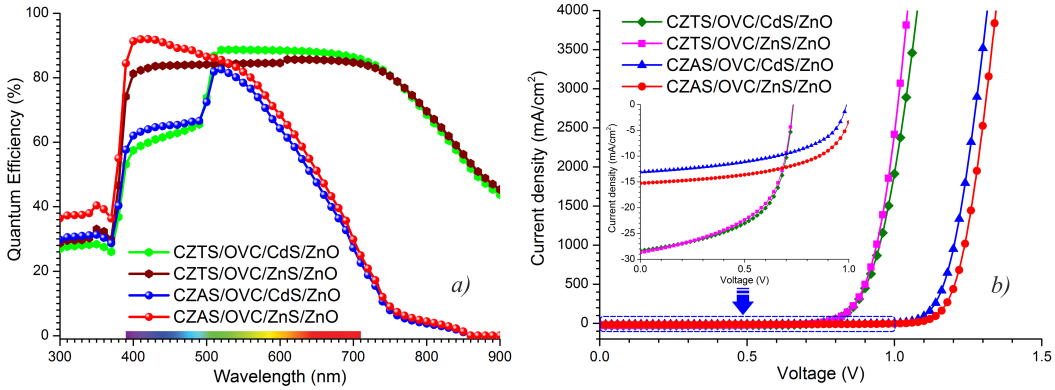

Figure 7. Comparison of quantum efficiency (a) and JV-characteristics (b) of TFSC CZTS, CZAS.

Conclusion

Thus, in this work, within the framework of the Poisson equation, the main parameters and characteristics of the TFSC based on the non-toxic multicomponent semiconductor compound $CuZn_2AlS_4$ are determined. Quantum efficiency, CVC, open-circuit voltage, short-circuit current, fill factor, efficiency of the TFSC based on CZAS have been calculated. It has been established that the minimum optimum thickness of the CZAS absorber is 1-1.25 microns and a further increase in the absorber's thickness insignificantly affects the energy characteristics and the main parameters. It was revealed that with an increase in the operating temperature (280-400 K), the performance of the TFSC deteriorates, the efficiency of the model TFSC rapidly drops from 9.2% (at 280 K) to 5.47% (at 400 K). The results of a comparison of the quantum efficiency and CVC of model TFSCs

based on CZTS/CdS, CZTS/ZnS and CZAS/CdS, CZAS/ZnS are presented. It is shown that in the wavelength range of 390-500 nm, CZAS-based TFSC has a high quantum efficiency, but in the range of 540-900 nm it is significantly inferior to CZTS. This allows CZAS to be used as a photovoltaic material for creating multi-junction solar cells designed to absorb solar radiation in the 390-500 nm range. It has been found that the combination of CZAS films with a ZnS buffer layer improves TFSC performance.

Acknowledgments

This work was supported by grant of the Ministry of Education and Science of the Republic of Kazakhstan AP09562784. The authors acknowledge the provision of SCAPS-1D software by Prof. Marc Burgelman.

References

[1] Y. Zhang et al., Solar Energy Materials and Solar Cells **225** (2021) 111073.
[2] M. Bello et al., Journal of Alloys and Compounds **839** (2020) 155510.
[3] M. Hadadian et al., Energy and Environmental Science **13** (2020) 1377-1407.
[4] N. Ali et al., Materials Science in Semiconductor Processing **107** (2020) 104810.
[5] I. Kaulachs et al., Latvian Journal of Physics and Technical Sciences **1** (2021) 53-69.
[6] X. Zeng et al., Optics Letters **46** (2021) 2288-2291.
[7] W. Witte et al., ECS Journal of Solid State Science and Technology **10** (2021) 055006.
[8] H. Yang et al., Materials **14** (2021) 2413.
[9] S. Ishizuka et al., Journal of Applied Physics **106** (2009) 034908.
[10] P. Reinhard et al., Solar Energy Materials and Solar Cells **119** (2013) 287-290.
[11] A. Kumar et al., Superlattices and Microstructures **153** (2021) 106872.
[12] J. Xu et al., Materials **115** (2021) 111034.
[13] G. Anima et al., New Journal of Chemistry **40** (2016) 1149-1154.
[14] G.F. Novikov et al., Phys. Usp. **60** (2017) 161-178.
[15] R. Jacob et al., Phys. Status Solidi A **209** (2012) 2195-2200.
[16] M. Burgelman et al., Thin Solid Films **361-362** (2000) 527-532.
[17] K. Decock et al., Journal of Applied Physics **111** (2000) 043703.
[18] M. Burgelman et al., Thin Solid Films **535** (2000) 296-301.
[19] K. Decock et al., Thin Solid Films **519** (2011) 7481-7484.
[20] V.A. Milichko et al., Phys. Usp. **59** (2016) 727-772.